

Facial Synthesis of Carrageenan/Reduced Graphene Oxide/Ag Composite as Efficient SERS Platform

Yuhong Zheng^{a*}, Aiwu Wang^b, Zhong Wang^a, Li Fu^a, Feng Peng^a

^a Institute of Botany, Jiangsu Province and Chinese Academy of Sciences, Nanjing Botanical Garden, Memorial Sun Yat-Sen, Nanjing 210014, China

^b Department of Physics and Materials Science, City University of Hong Kong, Hong Kong

Received: April 8, 2016; Revised: September 17, 2016; Accepted: October 20, 2016

In this paper, we reported the preparation of carrageenan/reduced graphene oxide/Ag composite (CA-RGO-Ag) by a wet chemical method at room temperature using carrageenan, graphene oxide and silver nitrate as starting materials. As-prepared composite was characterized by UV-vis spectroscopy, Raman spectroscopy, FTIR, SEM, EDX and XRD. Results showed that the reduction of graphene oxide (GO) and silver nitrate was achieved simultaneously by addition of NaBH₄. Surface-enhanced Raman scattering study showed that the obtained composite give an intensive and enhanced Raman scattering when Rhodamine B was used as a probing molecule.

Keywords: Composite, Ag NPs, SERS, Graphene, Carrageenan, Adenine

1. Introduction

Surface enhanced Raman scattering (SERS) is a powerful analytical tool that can provide ultrasensitive detection of chemical and biological molecules down to the single molecular level, which has been used in various fields of chemistry, material science and biophysics¹. There are two SERS mechanisms that are generally accepted: electromagnetic mechanism (EM) and chemical mechanism (CM)²⁻⁴. EM is based on the enhancement of the local electromagnetic field while the CM is based on charge transfer between absorbed molecules and substrate surface. Up to now, many surfaces have been successfully investigated as SERS active substrates such as Ag, Au, Cu, Na, Li, Pd, Pt, the best performances for detection purposes have been recorded in the case of Ag and Au nanoparticles⁵⁻¹⁶.

Graphene, a two-dimensional monolayer sheet of hexagonal carbon atoms, has attracted great attention because of its unique structure and exceptional physiochemical properties¹⁷⁻²⁰. It has previously been reported to play a role as a Raman enhancement substrate because target molecules can easily form a unified orientation on it due to the flatness of the graphene surface^{21,22}. Moreover, the interconnected sp² network of graphene gives it the ability to undergo π - π stacking with aromatic molecules^{23,24}. However, most of the graphene used for preparing SERS substrate are in its reduced form from graphene oxide (GO) prepared by the oxidation of graphite. The reduced graphene oxide (RGO) is prone to irreversible spontaneous agglomeration, which highly limits its applications and performances^{25,26}. Therefore, surface functionalization is considered as an effective way

to solve this problem²⁷⁻³¹. In this report, we prepared an enhanced sensitivity for SERS detection using carrageenan functionalized RGO-Ag (CA-RGO-Ag) composite. The prepared composite was characterized by a series of techniques and its SERS property was evaluated by the detection of Rhodamine B (RhB) and adenine.

2. Experimental

2.1 Materials

Synthetic graphite (average particle diameter <20 μm), Rhodamine B (RhB), adenine, silver nitrate (AgNO₃), k-carrageenan and sodium borohydride (NaBH₄) were purchased from Sigma-Aldrich. All other chemicals used were analytical grade reagents without further purification. Milli-Q water (18.2 M Ω cm) was used throughout the experiments.

2.2 Synthesis of CG/RGO/Ag composite

Graphene oxide was prepared using modified Hummer's method^{32,33}. In a typical procedure, 125 ml of concentrated sulfuric acid was taken into a flask filled with graphite powder (5 g) followed by the addition of KMnO₄ (17.5 g) slowly at 0 °C. The mixture was stirred for 3 h at 35 °C and then diluted by water at 0 °C. After that, H₂O₂ (30 vol.% in water) was added into mixture until the bubbling of the gas was completed. The graphene oxide (GO) powder was collected by centrifugation of the solution and subsequently dried under vacuum at 80 °C for 24 h.

To synthesize CG/RGO/Ag composite, 0.5 mg carrageenan was dissolved into 50 mL water by 30 min sonication to form a brown solution. 10 mL GO dispersion (1 mg/mL) was

* e-mail: yuhongzhengcas@gmail.com

added into carrageenan solution for 1 h stirring. After that, a certain amount of AgNO_3 solution (50 mM) was added into the mixture for another hour stirring. Then, 1 mL NaBH_4 solution (0.5 M) was added to the above mixture dropwise. The color of the mixture turned from brown to black. After 30 min stirring, the composite was centrifuged, washed and dried at 80°C for 24 h. (denoted as CG/RGO/Ag-1, CG/RGO/Ag-2, CG/RGO/Ag-3, CG/RGO/Ag-4, CG/RGO/Ag-5 and CG/RGO/Ag-6 for the weight ratios of GO and AgNO_3 set as 1:5, 1:10, 1:20, 1:30, 1:40 and 1:50, respectively). CG/RGO and RGO/Ag sample also synthesized using a similar method except addition of AgNO_3 and carrageenan, respectively.

2.3 Characterizations

Surface morphology of samples were analyzed by scanning electron microscope (SEM, S-4700, HITACHI). FTIR spectra were obtained using a Nicolet 8700 FTIR spectrometer (Thermo Scientific Instrument). X-ray diffraction patterns were collected from 10° to 60° in 2θ by a XRD with $\text{Cu K}\alpha$ radiation (D8-Advanced, Bruker). Raman analysis was carried out at room temperature using a Raman spectroscopy (Renishaw InVia, UK) with a 514 nm laser light. The optical characterizations were obtained by UV-vis spectrophotometer in the wavelength range from 200 to 500 nm.

2.4 SERS study

For SERS study, 20 μL of CA-RGO-Ag dispersion was dropped onto the glass substrate and dried at room temperature. Then, 20 μL of 1.0×10^{-4} M ethanol solution was dropped onto the CA-RGO-Ag films and dried at room temperature, and SERS spectra were recorded, respectively.

3. Results and Discussion

UV-vis spectroscopy was used for confirming the formation of Ag nanoparticles (NPs) and reduction of GO. Figure 1A displays the UV-vis spectra of GO and CA-RGO-Ag composite. It can be seen that the spectrum of GO exhibits two characteristic absorption peaks at 227 nm and 315 nm, corresponding to $\pi-\pi^*$ transitions of aromatic C—C bonds and $n-\pi^*$ transitions of C=O bonds, respectively³⁴. However, the peak at 227 nm of GO dispersion gradually red-shifts to 262 nm and the shoulder absorption peak at 316 nm disappear in the spectrum of CA-RGO-Ag-6, which indicates the GO has been reduced by NaBH_4 . Furthermore, a new broad absorption peak at 425 nm is observed in the spectrum of CA-RGO-Ag-6, which could assign to the surface plasmon resonance absorption band of Ag nanoparticles, suggesting the successful formation of Ag NPs.

Figure 1B displays the FTIR spectra of GO and CA-RGO-Ag-6. As expected, the spectrum of GO exhibits signals at 3432, 1638, 1156 and 1038 cm^{-1} corresponding to the

—OH vibration stretching, carboxyl C=O, epoxy C—O and alkoxy C—O, respectively³⁵. It can be seen that these peaks show a relatively lower intensity or even vanished in the spectrum of CA-RGO-Ag-6, further confirm the reduction of GO. Moreover, the spectrum of CA-RGO-Ag-6 also shows peaks at 1225, 915 and 852 cm^{-1} , which could be assigned as the characteristic peaks of carrageenan, suggesting the successful surface functionalization of carrageenan^{36,37}.

Raman spectroscopy was also used for determining the structural changes of the as-prepared samples. The Raman spectra of graphite, GO and CA-RGO-Ag-6 are shown in Figure 2. As expected, a prominent peak at 1580 cm^{-1} is observed in graphite sample, which corresponds to the first-order scattering of the E_{2g} . The spectrum of GO displays two characteristic main peaks for D band at 1330 cm^{-1} and G bands at 1585 cm^{-1} . The G band is attributed to all sp^2 carbon forms and provides information on the in-plane vibration of sp^2 bonded carbon atoms while the D band suggests the presence of sp^3 defects³⁸. The intensity ratio between D band and G band (I_D/I_G) increases from 0.91 in GO to 1.1 in CA-RGO-Ag-6 is due to the decrease of average size of sp^2 domains by reduction of GO³⁹.

The morphology of as-prepared samples were examined by SEM. Figure 3A-H shows the top-view SEM images of RGO-Ag, CA-Ag, CA-RGO-Ag-1, CA-RGO-Ag-2, CA-RGO-Ag-3, CA-RGO-Ag-4, CA-RGO-Ag-5 and CA-RGO-Ag-6. It can be observed that the RGO-Ag (Figure 3A) exhibits a completely different morphology compared with carrageenan involved samples. The Ag NPs show an aggregated cluster form and touch on the RGO sheet surface. Compared with CA-RGO-Ag samples, the Ag NPs formed in the CA-Ag sample (Figure 3B) exhibits a much larger size. For CA-RGO-Ag samples, the RGO sheets are embedded into carrageenan gel. On the surface, we could observe a uniform distribution of single Ag nanoparticles when a higher AgNO_3 content was introduced during the preparation. The average size of the Ag NPs can be calculated to be 22 nm (for CA-RGO-Ag-5) based on 100 individual Ag NP size measurements. EDX analysis has been used to obtain elements information about CA-RGO-Ag-6 (Figure 4). The spectrum presents the only existence of C, O (belong to RGO), S (belongs to carrageenan) and Ag (belongs to Ag NPs), indicating the successful formation of composite with high purity.

The powder X-ray diffraction of the samples are shown in Figure 5. It is clear that the XRD pattern has peaks at 25.29° , which correspond to (002) crystal planes of graphite, indicating the presence of layered RGO sheets structure. Other diffraction peaks at 30.1° , 34.4° , 48.2° , 57.1° , 69.9° and 76.5° correspond to the (111), (200), (220), (311), (400) and (222) lattice planes of the Ag NPs, respectively.

RhB was chosen as the model molecule to examine the performance of CA-RGO-Ag SERS substrates. Figure 6 shows a set of the SERS spectra of 1×10^{-4} RhB on glass slide,

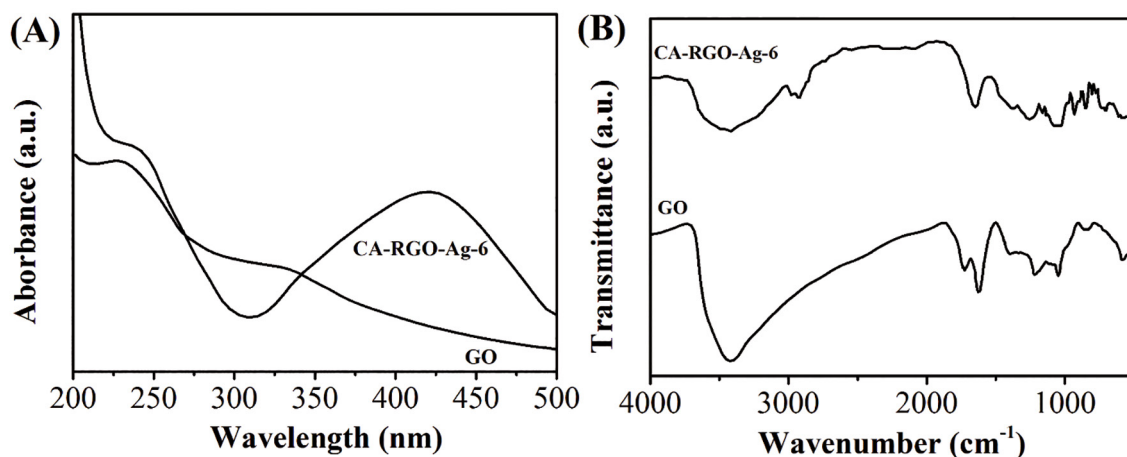


Figure 1: (A) UV-vis and (B) FTIR spectra of GO and CA-RGO-Ag-6.

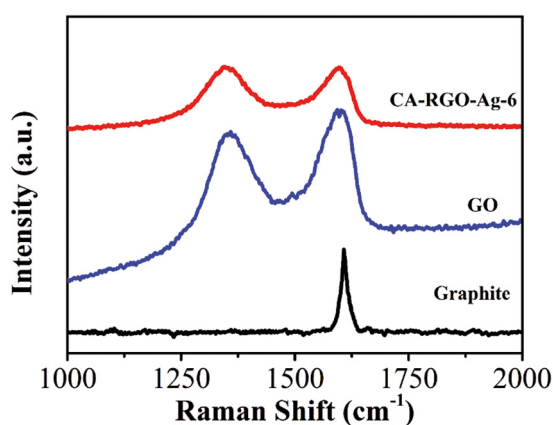


Figure 2: Raman spectra of graphite, GO and CA-RGO-Ag-6.

RGO-Ag and CA-RGO-Ag-3 substrates. It can be found that the 10^{-4} M RhB molecules alone (a) almost have no Raman signals. However, the spectra collected from RGO-Ag and CA-RGO-Ag-3 substrates all show distinct peaks at 624 (C—C ring in plane bend), 760 (C—H out of plane bend), 829 (C—C), 938 (C—H stretch), 1076 (β (CH)), 1191 (C—H in plane bend), 1277, 1362, 1502 (Arom C—H stretch), 1567, 1650 (Arom C—C stretch) and 1596 cm^{-1} (C—H stretch)⁴⁰⁻⁴². Compared SERS signals on RGO-Ag (b) with the ones on CA-RGO-Ag-2 (c), it can be found the SERS signal on CA-RGO-Ag-3 is stronger than the one on RGO-Ag, which could attract to both electromagnetic and chemical factors. As observed in the SEM characterizations, the introduction of carrageenan effectively prevents the formation of large cluster Ag NPs on the RGO sheets. The uniform distributed small Ag NPs play the role of electromagnetic hot spots that have intense local electromagnetic fields, resulting in highly efficient Raman scattering⁴³. On the other hand, the carrageenan surface functionalization could prevent the aggregation of RGO sheets, which could adsorb and concentrate the target molecules and magnify the SERS signal⁴⁴.

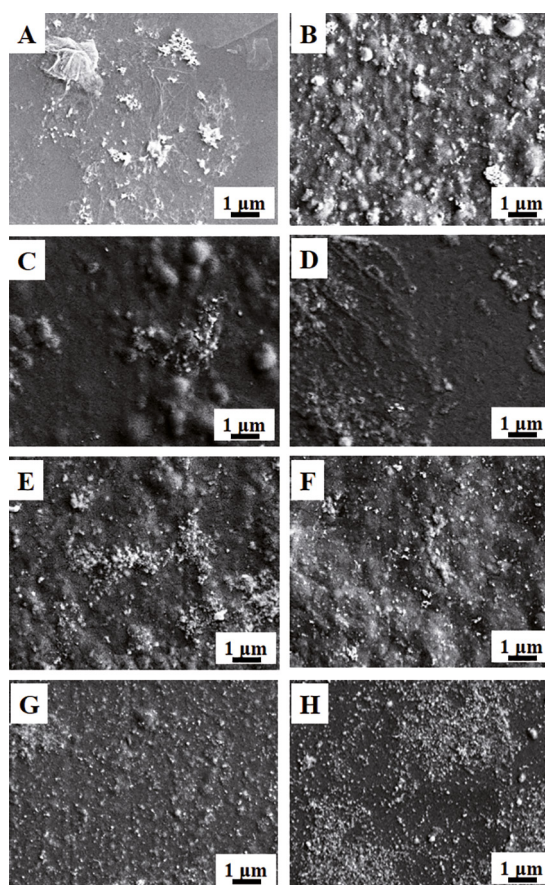


Figure 3: SEM images of (A) RGO-Ag, (B) CA-Ag, (C) CA-RGO-Ag-1, (D) CA-RGO-Ag-2, (E) CA-RGO-Ag-3, (F) CA-RGO-Ag-4, (G) CA-RGO-Ag-5 and (H) CA-RGO-Ag-6.

In order to optimize the performance, the SERS spectra were collected from the CA-RGO-Ag substrate with different composition. Figure 7 shows a set of the SERS spectra of 1×10^{-4} RhB on CA-RGO-Ag-1, CA-RGO-Ag-2, CA-RGO-Ag-3, CA-RGO-Ag-4, CA-RGO-Ag-6 and CA-RGO-Ag-5. From

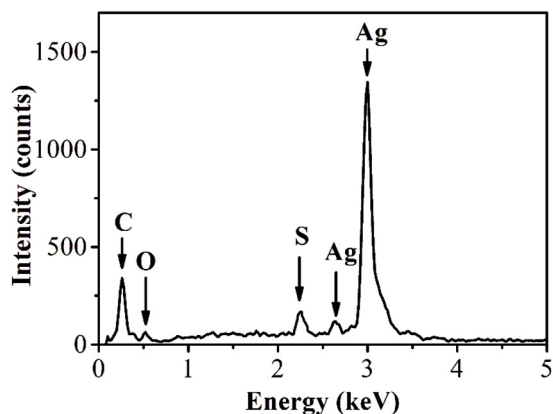


Figure 4: EDX spectrum of CA-RGO-Ag-6.

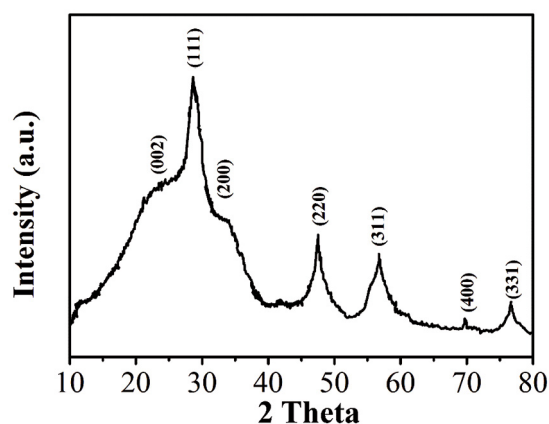


Figure 5: XRD pattern of CA/RGO/Ag-6.

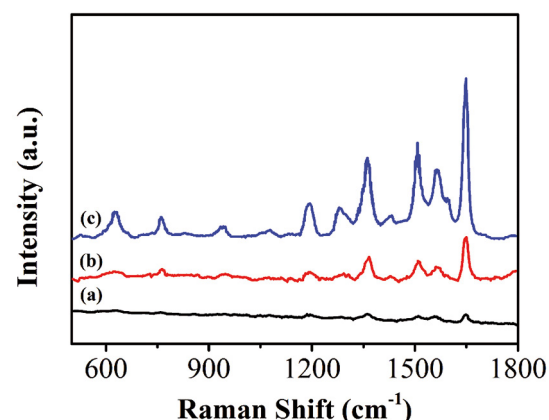


Figure 6: SERS spectra of (a) 10^{-4} M RhB molecules on glass reference surface, (b) 10^{-4} M RhB adsorbed on the RGO-Ag and (c) CA-RGO-Ag-3 substrates.

all the spectra, the SERS spectrum collected from CA-RGO-Ag-5 shows the highest enhancement performance, which could ascribe to the uniformity of Ag NPs distribution and optimized Ag NPs size adjusted by the interaction between Ag^+ and GO during the preparation process. Therefore, the

weight ratio of GO and AgNO_3 for fabricating CA-RGO-Ag SERS substrate was set as 1: 40.

The practical application of CA-RGO-Ag SERS substrate was tested by detection of adenine, a kind of nucleotide based for DNA sequencing. The SERS spectra of adenine (1×10^{-4} M) on the RGO-Ag and CA-RGO-Ag-5 are shown in Figure 8. It can be found that four characteristic peaks are pronounced at 730 , 1332 , 1444 and 1587 cm^{-1} , which are corresponded to the purine ring breathing mode, the C-N stretching mode, C-N in plane stretching mode and sciss NH_2 , respectively^{45,46}. Moreover, three peaks at 655 , 687 and 1054 cm^{-1} were also observed when using CA-RGO-Ag-5 as SERS substrate, indicating the proposed substrate exhibits an excellent SERS activity towards detection of adenine.

4. Conclusion

In conclusion, CA-RGO-Ag composite has been prepared via a facial wet chemical route using NaBH_4 as reducing agent. The as-prepared composite exhibits strong plasmonic resonances and can be used as a SERS substrate. The SERS

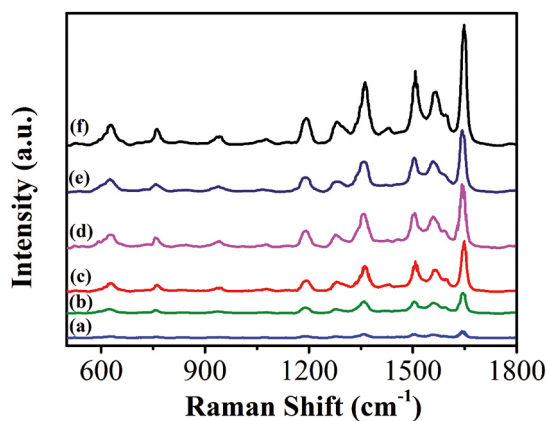


Figure 7: SERS spectra of 10^{-4} M RhB molecules on (a) CA-RGO-Ag-1, (b) CA-RGO-Ag-2, (c) CA-RGO-Ag-3, (d) CA-RGO-Ag-4, (e) CA-RGO-Ag-6 and (f) CA-RGO-Ag-5 substrates.

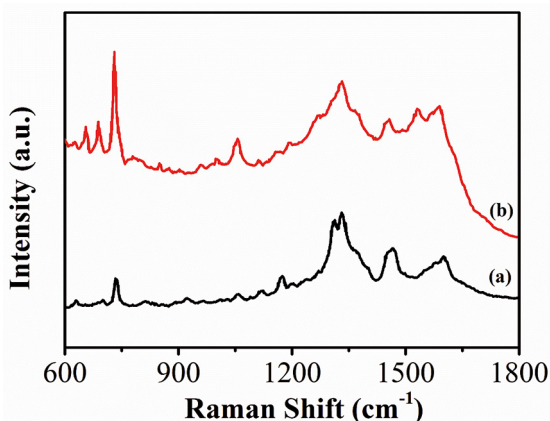


Figure 8: SERS spectra of 10^{-4} M adenine on (a) RGO-Ag and (b) CA-RGO-Ag-5 substrate.

activity of the CA-RGO-Ag substrate was optimized by varying the weight ratio of AgNO₃ and GO in the preparation process. The improved activity can be attributed to the uniform distributed small Ag NPs, which provides intense local electromagnetic fields, resulting in highly efficient Raman scattering. On the other hand, the carrageenan functionalized RGO sheets adsorb and concentrate the target molecules and magnify the SERS signal.

5. References

1. Tripp RA, Dluhy RA, Zhao Y. Novel nanostructures for SERS biosensing. *Nanotoday*. 2008;3(3-4):31-37.
2. Lombardi JR, Birke RL. A Unified View of Surface-Enhanced Raman Scattering. *Accounts of Chemical Research*. 2009;42(6):734-742.
3. Schwartzberg AM, Grant CD, Wolcott A, Talley CE, Huser TR, Bogomolni R, et al. Unique Gold Nanoparticle Aggregates as a Highly Active Surface-Enhanced Raman Scattering Substrate. *The Journal of Physical Chemistry B*. 2004;108(50):19191-19197.
4. Yoon I, Kang T, Choi W, Kim J, Yoo Y, Joo SW, et al. Single Nanowire on a Film as an Efficient SERS-Active Platform. *Journal of the American Chemical Society*. 2008;131(2):758-762.
5. Stiufluic R, Iacovita C, Lucaciu C, Stiufluic G, Dutu A, Braescu C, et al. SERS-active silver colloids prepared by reduction of silver nitrate with short-chain polyethylene glycol. *Nanoscale Research Letters*. 2013;8:47.
6. Otsuka H, Nagasaki Y, Kataoka K. PEGylated nanoparticles for biological and pharmaceutical applications. *Advanced Drug Delivery Reviews*. 2003;55(3):403-419.
7. Hameed A, Khan I, Azam A, Naz SS, Khan A, Saleem M, et al. Stability and enzyme inhibition activities of Au nanoparticles using an aqueous extract of clove as a reducing and stabilizing agent. *Journal of the Chemical Society of Pakistan*. 2014;36(3):542-547.
8. Piergies N, Kim Y, Proniewicz E. Potential-dependant SERS interaction of ortho-substituted N-benzylamino(boronphenyl) methylphosphonic acid with Ag, Au, and Cu electrode surfaces. *Vibrational Spectroscopy*. 2016;83:94-100.
9. Guo M, Zhao Y, Zhang F, Xu L, Yang H, Song X, et al. Reduced graphene oxide-stabilized copper nanocrystals with enhanced catalytic activity and SERS properties. *RSC Advances*. 2016;6(56):50587-50594.
10. Li R, Yang G, Yang J, Han J, Liu J, Huang M. Determination of melamine in milk using surface plasma effect of aggregated Au@SiO₂ nanoparticles by SERS technique. *Food Control*. 2016;68:14-19.
11. Guo TL, Li JG, Sun X, Sakka Y. Improved galvanic replacement growth of Ag microstructures on Cu micro-grid for enhanced SERS detection of organic molecules. *Materials Science and Engineering: C*. 2016;61:97-104.
12. Kang T, Jeong S, Kang H, Kim J, Kim HM, Kyeong S, et al. Fabrication of Ag nanoaggregates/SiO₂ yolk-shell nanopores for surface-enhanced Raman scattering. *Journal of Industrial & Engineering Chemistry*. 2015;32:34-38.
13. Šubr M, Petr M, Peksa V, Kylián O, Hanuš J, Procházka M. Ag Nanorod Arrays for SERS: Aspects of Spectral Reproducibility, Surface Contamination, and Spectral Sensitivity. *Journal of Nanomaterials*. 2015;2015:729231.
14. Cui L, Chen S, Zhang K. Effect of toxicity of Ag nanoparticles on SERS spectral variance of bacteria. *Spectrochimica Acta Part A: Molecular and Biomolecular Spectroscopy*. 2015;137:1061-1066.
15. Khlebtsov BN, Liu Z, Ye J, Khlebtsov NG. Au@Ag core/shell cuboids and dumbbells: Optical properties and SERS response. *Journal of Quantitative Spectroscopy & Radiative Transfer*. 2015;167:64-75.
16. Lai W, Zhou J, Liu Y, Jia Z, Xie S, Petti L, et al. 4MBA-labeled Ag-nanorod aggregates coated with SiO₂: synthesis, SERS activity, and biosensing applications. *Analytical Methods*. 2015;7(20):8832-8838.
17. Xu Y, Liu Z, Zhang X, Wang Y, Tian J, Huang Y, et al. A Graphene Hybrid Material Covalently Functionalized with Porphyrin: Synthesis and Optical Limiting Property. *Advanced Materials*. 2009;21(12):1275-1279.
18. Wang D, Choi D, Li J, Yang Z, Nie Z, Kou R, et al. Self-Assembled TiO₂-Graphene Hybrid Nanostructures for Enhanced Li-Ion Insertion. *ACS Nano*. 2009;3(4):907-914.
19. Yoo E, Kim J, Hosono E, Zhou H, Kudo T, Honma I. Large Reversible Li Storage of Graphene Nanosheet Families for Use in Rechargeable Lithium Ion Batteries. *Nano Letters*. 2008;8(8):2277-2282.
20. Ma XY, Chen MF, Chao MY. Voltammetric Determination of Sudan II in Food Samples at Graphene Modified Glassy Carbon Electrode Based on the Enhancement Effect of Sodium Dodecyl Sulfate. *Journal of the Chemical Society of Pakistan*. 2013;35(1):30-36.
21. Ling X, Xie L, Fang Y, Xu H, Zhang H, Kong J, et al. Can Graphene be used as a Substrate for Raman Enhancement? *Nano Letters*. 2009;10(2):553-561.
22. Jung N, Crowther AC, Kim N, Kim P, Brus L. Raman Enhancement on Graphene: Adsorbed and Intercalated Molecular Species. *ACS Nano*. 2010;4(11):7005-7013.
23. Wojcik A, Kamat PV. Reduced Graphene Oxide and Porphyrin. An Interactive Affair in 2-D. *ACS Nano*. 2010;4(11):6697-6706.
24. Emery JD, Wang QH, Zarrouati M, Fenter P, Hersam MC, Bedzyk MJ. Structural analysis of PTCDA monolayers on epitaxial graphene with ultra-high vacuum scanning tunneling microscopy and high-resolution X-ray reflectivity. *Surface Science*. 2011;605(17-18):1685-1693.
25. Wang G, Shen X, Wang B, Yao J, Park J. Synthesis and characterisation of hydrophilic and organophilic graphene nanosheets. *Carbon*. 2009;47(5):1359-1364.
26. Kochnev AS, Ovid'ko IA, Semenov BN. Tensile strength of graphene containing 5-8-5 defects. *Reviews on Advanced Materials Science*. 2014;37(1-2):105-110.
27. Liu H, Cheng J, Chen F, Hou F, Bai D, Xi P, et al. Biomimetic and cell-mediated mineralization of hydroxyapatite by carrageenan functionalized graphene oxide. *ACS Applied Materials & Interfaces*. 2014;6(5):3132-3140.

28. Liu S, Bao H, Li L. Thermoreversible gelation and scaling laws for graphene oxide-filled κ -carrageenan hydrogels. *European Polymer Journal*. 2016;79:150-162.
29. Wang J, Ouyang Z, Ren Z, Li J, Zhang P, Wei G, et al. Self-assembled peptide nanofibers on graphene oxide as a novel nanohybrid for biomimetic mineralization of hydroxyapatite. *Carbon*. 2015;89:20-30.
30. Zhu D, Nakamura H, Zhu H, Xu C, Matsuo M. Microfibers from interpolymer complexation of κ -carrageenan and oligomers of polyaniline for glucose detection. *Synthetic Metals*. 2015;202:133-139.
31. Song F, Li X, Wang Q, Liao L, Zhang C. Nanocomposite Hydrogels and Their Applications in Drug Delivery and Tissue Engineering. *Journal of Biomedical Nanotechnology*. 2015;11(1):40-52.
32. Park S, An J, Piner RD, Jung I, Yang D, Velamakanni A, et al. Aqueous Suspension and Characterization of Chemically Modified Graphene Sheets. *Chemistry of Materials*. 2008;20(21):6592-6594.
33. Hummers WS Jr., Offeman RE. Preparation of Graphitic Oxide. *Journal of the American Chemical Society*. 1958;80(6):1339.
34. Paredes JI, Villar-Rodil S, Martínez-Alonso A, Tascón JMD. Graphene Oxide Dispersions in Organic Solvents. *Langmuir*. 2008;24(19):10560-10564.
35. Liu Z, Robinson JT, Sun X, Dai H. PEGylated Nanographene Oxide for Delivery of Water-Insoluble Cancer Drugs. *Journal of the American Chemical Society*. 2008;130(33):10876-10877.
36. Zuo PP, Zhang YL, Feng HF, Xia W, Zhang WQ, Wang MZ. Fabrication and Properties of Graphene Oxide-reinforced Carrageenan Film. *Chemical Journal of Chinese Universities*. 2013;34(3):692-697.
37. Sun YJ, Wang CJ, Geng TF, Wang ZF, Huang LJ. Analysis of κ -Carrageenan Oligosaccharides by LC-ESI-MS/MSⁿ with 3-Amino-9-ethylcarbazole Derivatization. *Acta Chimica Sinica*. 2011;69(14):1697-1704.
38. Yang D, Velamakanni A, Bozkolu G, Park S, Stoller M, Piner RD, et al. Chemical analysis of graphene oxide films after heat and chemical treatments by X-ray photoelectron and Micro-Raman spectroscopy. *Carbon*. 2009;47(1):145-152.
39. Li X, Wang Q, Zhao Y, Wu W, Chen J, Meng H. Green synthesis and photo-catalytic performances for ZnO-reduced graphene oxide nanocomposites. *Journal of Colloid and Interface Science*. 2013;411:69-75.
40. Jung GB, Kim JH, Burm JS, Park HK. Fabrication of chitosan-silver nanoparticle hybrid 3D porous structure as a SERS substrate for biomedical applications. *Applied Surface Science*. 2013;273:179-183.
41. Yu X, Cai H, Zhang W, Li X, Pan N, Luo Y, et al. Tuning Chemical Enhancement of SERS by Controlling the Chemical Reduction of Graphene Oxide Nanosheets. *ACS Nano*. 2011;5(2):952-958.
42. Jung GB, Bae YM, Lee YJ, Ryu SH, Park HK. Nanoplasmonic Au nanodot arrays as an SERS substrate for biomedical applications. *Applied Surface Science*. 2013;282:161-164.
43. Inoue M, Ohtaka K. Surface enhanced raman-scattering by metal spheres. 1. Cluster effect. *Journal of the Physical Society of Japan*. 1983;52(11):3853-3864.
44. Ren W, Fang Y, Wang E. A Binary Functional Substrate for Enrichment and Ultrasensitive SERS Spectroscopic Detection of Folic Acid Using Graphene Oxide/Ag Nanoparticle Hybrids. *ACS Nano*. 2011;5(8):6425-6433.
45. Zhao H, Fu H, Zhao T, Wang L, Tan T. Fabrication of small-sized silver NPs/graphene sheets for high-quality surface-enhanced Raman scattering. *Journal of Colloid and Interface Science*. 2012;375(1):30-34.
46. Guo S, Li J, Ren W, Wen D, Dong S, Wang E. Carbon Nanotube/Silica Coaxial Nanocable as a Three-Dimensional Support for Loading Diverse Ultra-High-Density Metal Nanostructures: Facile Preparation and Use as Enhanced Materials for Electrochemical Devices and SERS. *Chemistry of Materials*. 2009;21(11):2247-2257.